Nano Energy 106 (2023) 108063

Contents lists available at ScienceDirect

Nano Energy

journal homepage: www.elsevier.com/locate/nanoen

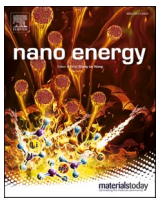

Photovoltaic-triboelectric hybridized nanogenerator for simultaneously scavenging light and liquid-droplet energies☆

Chengmin Bao [a,b,c,f], Huiyu Dan [a,b,e], Maoyi Zhang [b], Chuanbo Li [c,*], Zhong Lin Wang [b,d,e,**], Ya Yang [a,b,e,***]

[a] Center on Nanoenergy Research, School of Physical Science and Technology, Guangxi University, Nanning 530004, PR China
[b] CAS Center for Excellence in Nanoscience, Beijing Key Laboratory of Micro-Nano Energy and Sensor, Beijing Institute of Nanoenergy and Nanosystems, Chinese Academy of Sciences, Beijing 101400, PR China
[c] College of Life and Environmental Sciences, School of Science, Optoelectronic Research Center, Minzu University of China, Beijing 100081, PR China
[d] School of Material Science and Engineering, Georgia Institute of Technology, Atlanta, GA 30332-0245, USA
[e] School of Nanoscience and Technology, University of Chinese Academy of Sciences, Beijing 100049, PR China
[f] College of Chemistry and Environment, Hohhot Minzu College, Hohhot 010051, PR China

ARTICLE INFO

Keywords:
Hybridized nanogenerator
Triboelectric nanogenerator
Liquid-droplet energy
Light energy

ABSTRACT

Hybridized nanogenerator has made breakthroughs in multiple types of energy scavenging, however, introduction of new materials that make hybridized structure more simplified and environmentally friendly is needed further research. Here, we developed a hybridized nanogenerator composed of photovoltaic cell (PVC) and triboelectric nanogenerator (TENG), which can scavenge both light and liquid-droplet energies. In this device, the PVC share bottom electrode with the TENG. The device exhibits good hybridized process, generating peak current and peak voltage of 16.96 μA and 0.83 V, by scavenging light and liquid-droplet energies simultaneously. The hybridized output show that the maximum hybridized peak power was determined by the peak power of TENG who exhibited pulselike output, while the maximum hybridized output energy was much more affected by the output energy of PVC who generated continuous signals. This work enables the simultaneously scavenging light and liquid-droplet energies through individual device, which will open up unexplored avenues for simultaneously scavenging liquid-droplet energy and other types of energies.

1. Introduction

Triboelectric nanogenerator (TENG) has been widely used to scavenge ambient mechanical energy and convert into electric energy to meet the growing energy consumption in modern life [1–4]. However, as limited by the intended design, working condition or other factors, individual device is not available for multiple types of energy initially. To solve this issue, integrated device called as hybridized nanogenerator was designed for the purpose of obtaining a variety of energy sources. In these years, there have been many related researches about hybridized nanogenerator focusing on scavenging mechanical energy, vibration energy, solar energy, thermal energy, wave energy and so on through various effective units [5–15].

Besides, with regard to the friction interfaces, in addition to solid-solid TENG, research on other types of TENG between liquid-liquid, liquid-gas, solid-gas and solid-liquid interface were well developed recently [16–18]. In 2014, a water-TENG to harvest the water-related energy at liquid-solid interface was firstly developed [19]. After that a transistor-like droplet based electric generator (DEG) whose output performance was much more better than traditional solid-liquid

☆ "Prof Zhong Lin Wang, an author on this paper, is the Editor-in-Chief of Nano Energy, but he had no involvement in the peer review process used to assess this work submitted to Nano Energy. This paper was assessed, and the corresponding peer review managed by Professor Chenguo Hu, also an Associate Editor in Nano Energy"

* Corresponding author.
** Corresponding author at: CAS Center for Excellence in Nanoscience, Beijing Key Laboratory of Micro-Nano Energy and Sensor, Beijing Institute of Nanoenergy and Nanosystems, Chinese Academy of Sciences, Beijing 101400, PR China.
*** Corresponding author at: Center on Nanoenergy Research, School of Physical Science and Technology, Guangxi University, Nanning 530004, PR China.
E-mail addresses: cbli@muc.edu.cn (C. Li), zhong.wang@mse.gatech.edu (Z.L. Wang), yayang@binn.cas.cn (Y. Yang).

https://doi.org/10.1016/j.nanoen.2022.108063
Received 23 September 2022; Received in revised form 14 November 2022; Accepted 28 November 2022
Available online 2 December 2022

generator was proposed in 2020 [20]. Since then many researches followed this work was reported, focusing on the fabrication of the water-solid TENG based on various materials [21,22] and different structure [23–26], or simultaneously collecting other types of energies while collecting liquid-droplet energy [27–29]. Among them, the hybridized generator scavenging both light and liquid-droplet energies has attracted researchers' attentions a lot since it has a good application scenario that can work under any weather conditions in sunny or rainy days. So far, a number of studies have been demonstrated to integrate solar cells with conventional single-electrode liquid-droplet TENG to scavenge solar and raindrop energies simultaneously [30–33]. However, the reported two energy harvesters are just simply stacked together, without considering the effect of the solar energy harvester on the output performance of the TENG. In addition, the TENG used a conventional single electrode model with low and uncompetitive output current. With the development of emerging solar cells, researchers' interest was gradually shifting away from conventional p-n junction solar cells due to their excessive light-absorbing layer thickness and high cost [34]. Some new ideas for the study of hybridized nanogenerators are realized for scavenging light and liquid-droplet energies. A perovskite solar cell with a transistor-like liquid-droplet TENG has been used to enable the scavenging of two types of energies [27], where the MoO_3 layer was used in the TENG for enhancing the corresponding output performance. However, the two energy harvesters are still two relatively independent units, with more total layers of the device and a more complex structure are needed. Perovskite solar cells contained toxic Pb which may have the potential impact of environmental pollution. Thus, these materials with the properties of thin, low cost and environmentally friendly while the material also has good dielectric property for increasing the charge density of the TENG friction layer, are needed for the further development of the photovoltaic-triboelectric hybridized nanogenerators. If ferroelectric thin film can be used in the liquid-droplet TENG, the excellent photovoltaic property can be used for scavenging light energy [35–37]. Meanwhile, the superior dielectric performance of the ferroelectric thin film can be used to increase the surface charges of the TENG. The use of ferroelectric thin film dielectric layer will allow the hybridized device to efficiently integrate two individual energy harvesters and enable simpler hybridized device structure.

In this work, we developed a hybridized nanogenerator consisting of a photovoltaic cell (PVC) and a TENG, that can scavenge both light energy and liquid-droplet energy. The $BaTiO_3$ (BTO) film was introduced to a liquid-droplet energy scavenging TENG to retain the surface charges. Meanwhile, the PVC share the bottom electrode with the TENG. The device exhibits good hybridized process, generating peak current of 16.96 μA and peak voltage of 0.83 V, by scavenging both light and liquid-droplet energies simultaneously. The maximum peak power density can reach 3.71 mW/m^2, and the maximum output energy density reached 15.36 mJ/m^2. The maximum hybridized peak power was determined by the peak power of TENG who exhibited pulse-like output, while the maximum hybridized output energy was much more affected by the output energy of PVC who generated continuous signals. This work enables simultaneously scavenging light and liquid-droplet energies through individual device, which will open up unexplored avenues for hybridizing TENG and other ferroelectric films to scavenge liquid-droplet energy and other types of energies simultaneously.

2. Experimental section

2.1. Preparation of $BaTiO_3$ (BTO) solution

A certain molar ratio of barium acetate was dissolved in ultra pure water, glacial acetic acid and ethanol. To obtain solution 1, the solution above was stirred at 70 ℃ until it became clear. Then to obtain solution 2, a certain molar ratio of tetrabutyl titanate was taken in a container, with a certain amount of ethanol, glacial acetic acid and acetylacetone added in it, and the solution above was stirred for 30 min at room temperature. Finally, to obtain 0.1 mol/L clarified light yellow BTO colloid, solution 2 was added to solution 1 drop by drop then aged for 24 h.

2.2. Preparation of $LaNiO_3$ (LNO) solution

A certain molar ratio of nickel acetate and lanthanum nitrate were taken in a container, dissolved in glacial acetic acid and stirred at room temperature to obtain a clear solution, then continued to add ethanol in it and stir. Finally a 0.3 mol/L green transparent solution was obtained.

2.3. Fabrication of the device

A piece of 30 mm × 30 mm × 0.5 mm Si substrate was cleaned in acetone and ethanol for 5 min respectively using ultrasonic cleaning. The LNO solution was spin coated 6 layers onto the Si substrate and used as bottom electrode. Each layer of the LNO solution was heated in proper order at 180 ℃ for 3 min, 400 ℃ for 3 min and 700 ℃ for 3 min after spin coating to evaporate residual solvents and to anneal. Then the BTO solution was spin coated 6 layers onto the LNO. Each layer of the BTO solution was heated in proper order at 180 ℃ for 5 min, 400 ℃ for 5 min and 700 ℃ for 5 min after spin coating. After the BTO/LNO film was obtained, a layer of 2 mm × 2 mm × 50 μm indium tin oxide (ITO) film was fabricated on the BTO/LNO film by magnetron sputtering with 150 W at room temperature. Then a layer of 30 mm × 30 mm × 30 μm fluorinated ethylene propylene (FEP) film was glued on the prepared BTO/LNO which was sputtered with ITO on it. The Last Step was the fabrication of the top electrode, a piece of 1 mm × 12 mm × 30 μm Al foil whose position should not cover the ITO film was adhered onto the FEP film.

2.4. Characterization and measurements

The morphologies of BTO film surface and the cross-sectional image of the photovoltaic cell (PVC) were characterized using scanning electron microscope (Hitachi SUS8020). A 365 nm light-emitting diode (LED) is used as the light source, whose distance from the ITO surface is 2.5 cm. The light intensity was measured by a power meter (OPHIR Starlite). A beaker filled with water was placed on an iron support stand whose height can be facilely adjusted. A plastic tube and a syringe pump were used to pump water droplets from the beaker. The dropping frequency of water droplet was adjusted by the syringe pump. A nozzle whose diameter can be varied was connected to the plastic tube, so the volume of each droplet can also be tuned. Ultra pure water (electrical resistivity was 18 MΩ·cm), pure water (electrical conductivity was 12.6 μs/cm), tap water or salt solution (NaCl concentration was 3.5 %) were used according to the experimental conditions. The device was glued on an acrylic plate which was tilted on an acrylic trapezoid block with different angle of inclination. The electrical signals of hybridized device and TENG were characterized with a Keithely 6514 electrometer controlled by a computer. The electrical signals of PVC were characterized with a Keithely 2611B controlled by a computer.

3. Results and discussion

3.1. Output performance of the device

To scavenge light energy and liquid-droplet energy together through individual device, we assembled a hybridized nanogenerator that can scavenge both two types of energy simultaneously or separately, which is shown in Fig. 1a,b and Fig. S1a,b. The device was made of six layers as shown in Fig. 1c, Si substrate layer, $LaNiO_3$ (LNO) electrode layer, $BaTiO_3$ (BTO) film layer, ITO electrode layer, FEP film layer and Al electrode layer, from the bottom to the top. The LNO electrode layer, BTO film layer and ITO electrode layer constituted the PVC to scavenge

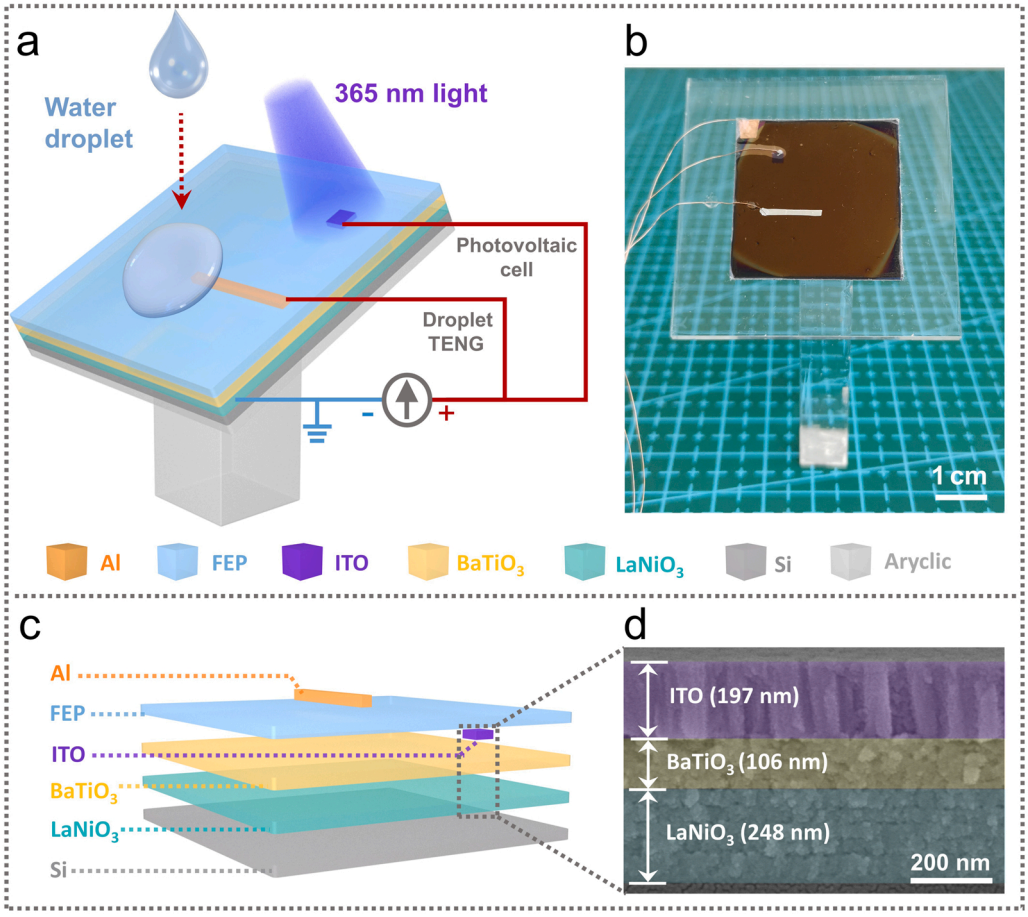

Fig. 1. Schematic diagram of the hybridized nanogenerator. (**a**) Schematic diagram and (**b**) optical image of the hybridized generator. (**c**) Schematic diagram of the cross-sectional of the hybridized generator.(**d**) The cross-sectional SEM image of the PVC.

light energy, in which the ITO layer acted as the top electrode and the LNO layer acted as the bottom electrode. Fig. 1d shows the cross-sectional image of PVC, Fig. S1c shows the surface morphology of BTO film. The leftover FEP film layer and the Al electrode made up the TENG together with the LNO bottom electrode layer to harvest liquid-droplet energy. For the TENG, the Al electrode acted as the top electrode, and the LNO layer still acted as the bottom electrode. It is to say, the two functional units of the device share the bottom electrode together. When the light source was 365 nm LED, power density was 396 mW/cm^2, the average output current of the PVC was 2.65 μA and average output voltage was 0.40 V (Fig. 2a,b). While a 100 μL pure water droplet fell from a height of 50 cm, dropped on a 45° tilted device at a frequency of 4 Hz, the average peak current and peak voltage of the TENG were 14.94 μA and 0.73 V (Fig. 2a,b). When the light source and water droplet operated simultaneously, the average peak current and peak voltage of the hybridized nanogenerator were 16.96 μA and 0.83 V (Fig. 2a,b). Fig. 2a:I,b:I show the details of the hybridized electrical signals, contrasting with individual TENG signals in Fig. 2a:II,b:II. The transferred charges of the device are shown in Fig. S9, when the output current of the "PVC", "PVC + TENG" and "TENG" were 2.65 μA, 16.96 μA and 14.94 μA, the transferred charges in 5 s were 13.24 μC, 13.49 μC and 0.33 μC respectively. As the light source was continuously illuminated to produce a continuous current, the TENG output pulselike current. Therefore, even though the peak current of TENG was much higher than that of PVC, the accumulated charges transferred in a certain time period was much smaller than that of PVC.

To further examine how the PVC and TENG influence the hybridized nanogenerator performance, we measured and calculated the maximum peak power and output energy of the device. The current was tested under different load resistances. The power, power density, the energy and energy density were calculated according to the formula $P = I^2R$, $P/A = I^2R/A$, $E = \int I^2Rdt$ and $E/A = \int I^2Rdt/A$, respectively (A represents the device surface area). Fig. 2c shows the maximum peak power of the "PVC + TENG", "PVC" and "TENG". The maximum peak power were 3.34 μW, 0.22 μW and 3.05 μW at load resistance of 60 KΩ, 200 KΩ and 60 KΩ, respectively. Corresponding power density were 3.71 mW/m^2, 0.24 mW/m^2, 3.39 mW/m^2, respectively. Fig. 2d shows the maximum output energy of the "PVC+TENG", "PVC" and "TENG". The maximum output energy were 13.82 μJ, 13.69 μJ, and 3.91 μJ at load resistance of 300 KΩ, 300 KΩ and 100 KΩ, respectively. Corresponding energy density were 15.36 mJ/m^2, 15.21 mJ/m^2, 4.34 mJ/m^2, respectively. The different characteristic between the maximum peak power and output energy can be found in these data. The maximum hybridized peak power was determined by the maximum peak power of the TENG, while the maximum hybridized output energy was much more affected by the maximum output energy of the PVC. This is because the water droplet dropped down at a certain frequency made the TENG presents a pulse-like output, and the peak current and voltage were much more higher than that of the PVC. While the output signals of the PVC was continuous because of the continuous illumination. Therefore, the output energy of the PVC calculated by integration was much higher than that of the TENG which was calculated by the same way.

Meanwhile, to verify how the PVC and TENG interact on each other, the signals shown in Fig. S2 were detected. Firstly, to determine how the BTO film affects the output performance of the TENG, the output performance of the device in Fig. S2a,b were measured. Compared with the device that have no BTO film between the LNO electrode and FEP film, the device who with BTO film shows good performance. The output

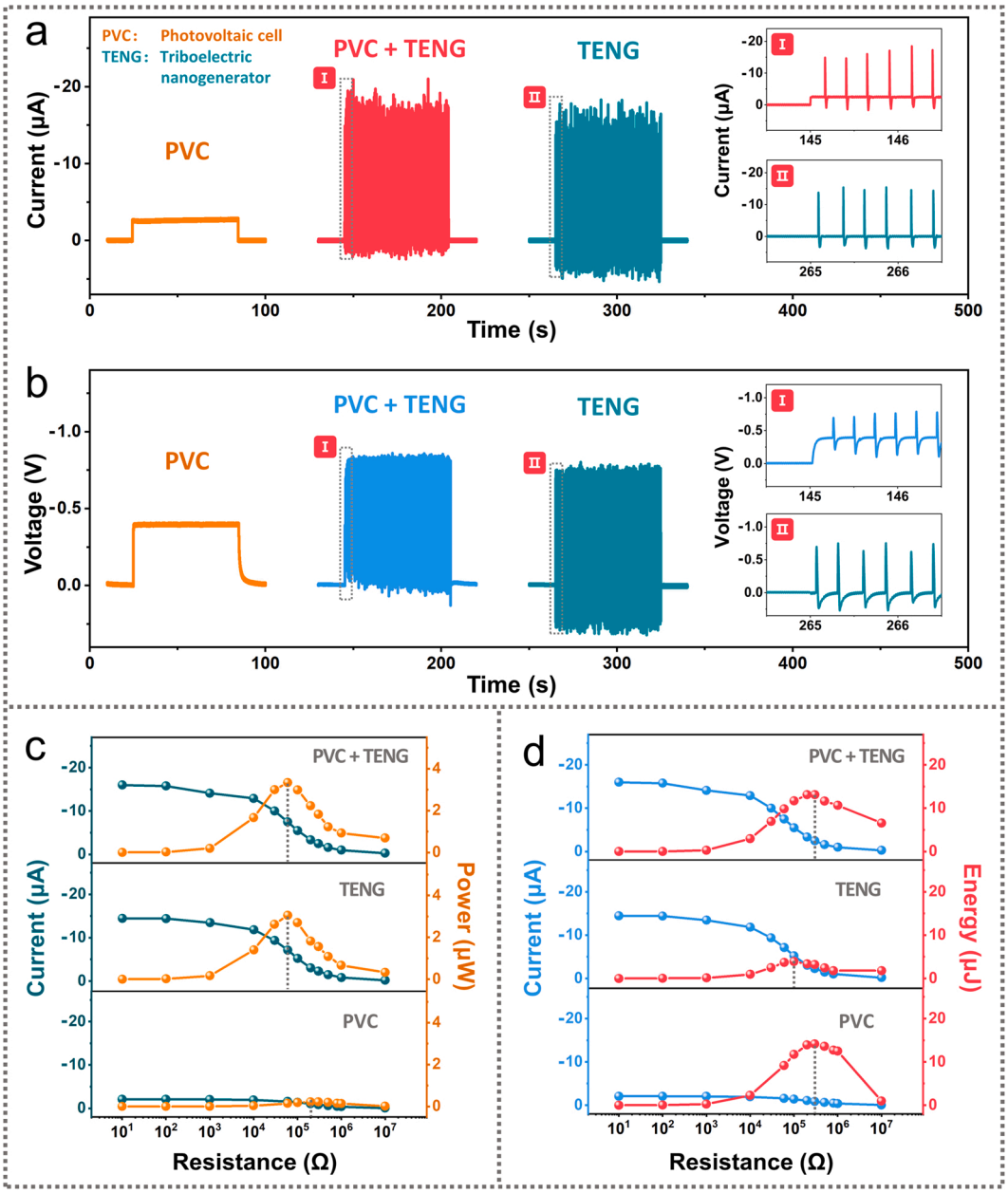

Fig. 2. Output performance of the hybridized nanogenerator. (a) The output current and (b) output voltage of the "PVC", "PVC + TENG" and "TENG". Insert I and II show details of the hybridized electric signals and individual TENG electric signals, respectively. (c) Load-dependent output current and peak power and (d) load-dependent output current and energy of the device relating to the "PVC + TENG", "TENG" and "PVC".

current and voltage of the unit without BTO film were 14.13 μA and 63.88 V, while the output current and voltage of the unit with BTO film were 18.70 μA and 77.49 V. Showing that the dielectric layer like BTO film between the friction layer (FEP film) and the bottom electrode (LNO film), increases the output performance of TENG owing to the charge storage properties [23,38]. The voltage of the device here in Fig. S2a,b was much higher than that in Fig. 2b whose voltage was no more than 0.87 V. The reason was because the circuit connection mode of sharing electrode as in Fig. 1 was equivalent to the TENG circuit and the PVC circuit connected in parallel. Thus the output voltage of the device was determined by the PVC circuit with BTO film's resistance of 1 MΩ which was much lower than TENG circuit with insulated FEP film. Secondly, the photovoltaic current and voltage of the device that with and without FEP film on the ITO film were tested respectively. Then it turned out that the output performance of the PVC much less affected by the FEP film (Fig. S2c,d). The photovoltaic current and voltage of the unit without FEP film were 2.54 μA and 0.28 V, while the photovoltaic current and voltage of the unit with FEP film were 2.47 μA and 0.27 V.

Fig. S3 shows the charging performance of the device which was connected to full wave rectifier including "PVC + TENG", "TENG" and "PVC". A capacitor of 4.7 μF could be charged up to 0.52 V, 0.45 V, 0.37 V by the "PVC + TENG", "TENG" and "PVC" respectively. Charging ability of each unit of the device follows the order of "PVC + TENG" > "TENG" > "PVC", which is consistent with the output voltage shown in Fig. 2b.

Working mechanism of the hybridized nanogenerator. The working mechanism of the hybridized nanogenerator can be divided into four steps, as shown in Fig. 3a. I: When there is no water droplet dropping on the device and no light source illuminating the ITO electrode, there will no charge transfers and no electrical signal appears; II: Once the water droplet contacted with the top Al electrode, the charges rapidly transfer from bottom to top electrode, generating a high transient output. At the

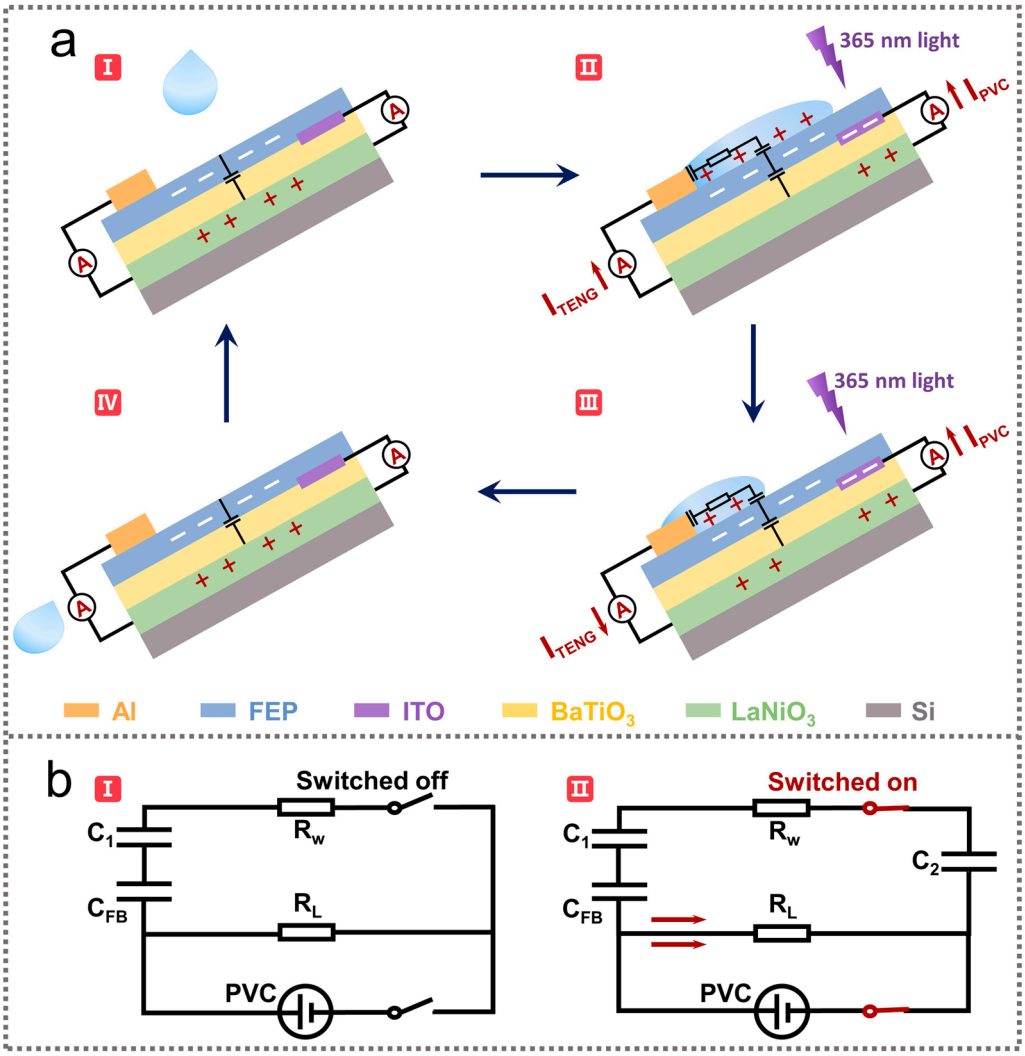

Fig. 3. Working mechanism of the hybridized nanogenerator. (**a**) Schematic diagram of the working mechanism of the hybridized nanogenerator. (I: No charge transfers; II: Charges transfer from bottom electrode to top electrode; III: Charges on C_2 flow back to bottom electrode, photo-generated charges transfer from bottom electrode to top electrode; IV: Return back). (**b**) Equivalent circuit model of the hybridized nanogenerator. (I: "switched-off" mode, II: "switched-on" mode).

same time, the light source acts on the device and the photo-generated charges transfer from the bottom electrode to the top; III: In the droplet retraction phase, the charges flow back to bottom electrode gradually until the droplet slides off from the top electrode. While the photo-generated charges still transfer from bottom electrode to the top electrode, during this stage; IV: Once the droplet slide off from the Al electrode and the light source stop illuminating, the device would return back to the initial state again.

The power generation process of the hybridized nanogenerator can be better explained with a equivalent circuit model in Fig. 3b. The droplet can be treated as a resistor, and the FEP with BTO together as a capacitor, C_{FB}, in which the LNO/BTO serves as the bottom plate while FEP/water as the top plate. Before the droplet drops on the top Al electrode, and the light doesn't illuminate, the circuit works in "switched-off" mode as shown in Fig. 3b:I. C_1, R_L, and R_W represent the capacitor at FEP/water interface, the external load resistance, and the water resistance. *PVC* represent the device's PVC part which is consisted of LNO layer, BTO layer and ITO layer. Once the droplet drops on the Al electrode, a capacitor C_2 formed at water/Al interface, switching the circuit into a closed circuit, as shown in Fig. 3b:II "switched-on" mode. In view of the thickness of the water/solid interface is several orders of magnitude thinner than that of the FEP with BTO, the capacitance of C_1, C_2 are dramatically higher than the capacitance of C_{FB}, according to the formula $C = \varepsilon S/d$, where C, ε, S and d are respectively the capacitance, the dielectric constant, plate area and plate distance of the capacitor. Besides, due to the high density surface charge stored in the FEP and BTO, U_1, U_2 (voltage across C_1, C_2) are negligible compared with U_{FB} (voltage across C_{FB}), based on the formula $C = Q/U$, where Q and U are respectively the charges of the capacitor and the voltage across the capacitor. Consequently, C_{FB} quick discharges to C_1, C_2, and presents an instantaneous peak output current from LNO to Al (Fig. S4). During this period, the voltage across C_1, C_2 increase with the charge accumulation. On the other hand, the capacitance of C_1, C_2 which decrease with the contact area reduction by the droplet sliding, increase the voltage across C_1, C_2 also. Therefore, once the voltage across C_1, C_2 exceed the voltage across C_{FB}, the capacitor C_{FB} is recharged by the capacitor C_1, C_2 in reverse (Fig. S4). The whole discharge and recharge process are activated when the water droplet drops on the Al electrode, and not stop until the water droplet slides off from the Al electrode. Meanwhile, for the PVC part, when the BTO film is in contact with the electrode, the energy bands at the interface of BTO/ITO and BTO/LNO are bent, forming a Schottky barrier. Under the illumination of 365 nm light source, the photo-generated electron-hole pairs are separated by the electric field of the Schottky junction at the interface. Due to the effect of the built-in electric field, the photo-generated electrons flow to the ITO side, and the photo-generated holes diffuse toward the LNO side. Thus

the output current from LNO to ITO can be detected in the external circuit (Fig. 3b:II).

Output performance of the hybridized nanogenerator under different parameters. It can be inferred that the capacitance *C* is closely related to the plate area *S* and the surface charge *Q*, based on the exposition above. The lager the contact area of the water droplet with the Al electrode, the bigger the capacitance, thus the greater the electric signals. Or the more the surface charges, the greater the electric signals. So the characterizations of the TENG under varied dripping height, droplet volume and dripping frequency were checked to prove this inference. As shown in Fig. 4a,b and Fig. S5a-d, the electric signals increase with the increase of droplet volume or dripping height except the condition of 220 cm. A larger droplet volume or dripping height leads to a larger droplet spreading area and a greater output. However for the condition of 220 cm height, splash or deflection of the droplet makes the contact area not large enough, so the signals were reduced at the point 220 cm. As shown in Fig. 4c and Fig. S5e,f, the output current and voltage increase with the increasing frequency of discrete droplet impingement and decrease in the case of continuous water flow. It can be explained that the surface charges are rapidly injected into a saturated state at high dripping frequency, which leads to a larger number of transferred charges [22]. But when the discrete droplet turns into continuous water flow, the surface charges cannot be transferred in time because of the continuous impact.

To further analyze the effect of other parameters, the output performance of the TENG under other different condition was tested, including tilted angle, dripping position, droplet ion concentration, width and length of the Al electrode. It can be observed that from Fig. 4d and Fig. S6a,b, the device tilted 45° exhibited the best performance than the device tilted at other angle. To define the effect of the dripping position, we measured the output performance of the device in Fig. 5a and Fig. S7a. The friction surface was divided into nine compartments and numbered. The output current and voltage were recorded when the droplet dropped at the each compartment. As shown in Fig. 5b,c and

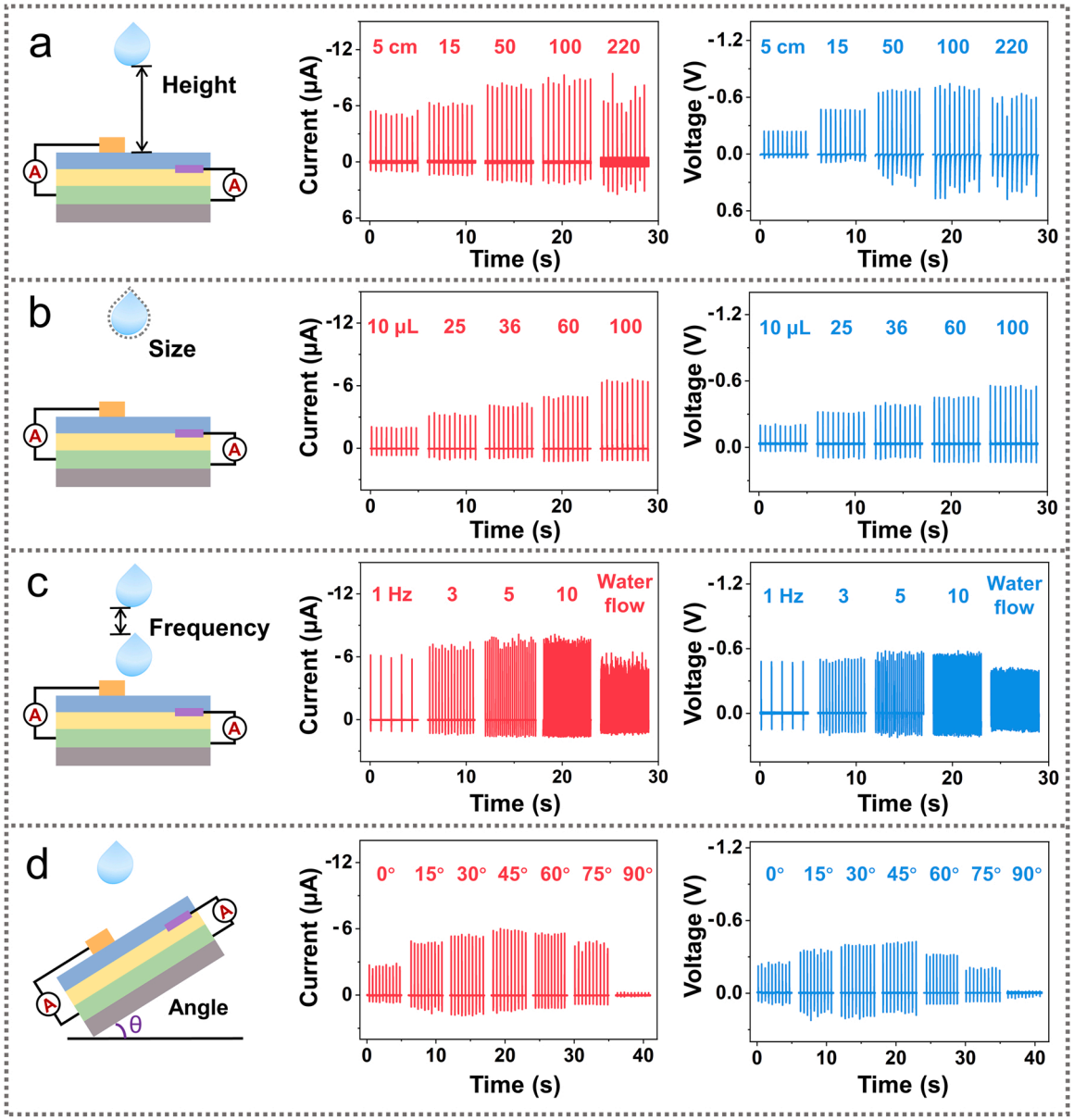

Fig. 4. Output performances of the TENG under different parameters. (a) The output current and voltage of the TENG under different heights (size = 60 μL, frequency = 2 Hz, angle = 45°), (b) different sizes (height = 15 cm, frequency = 2 Hz, angle = 45°), (c) different frequencies (height = 15 cm, size = 60 μL, angle = 45°) and (d) different angles (height = 15 cm, size = 60 μL, frequency = 2 Hz).

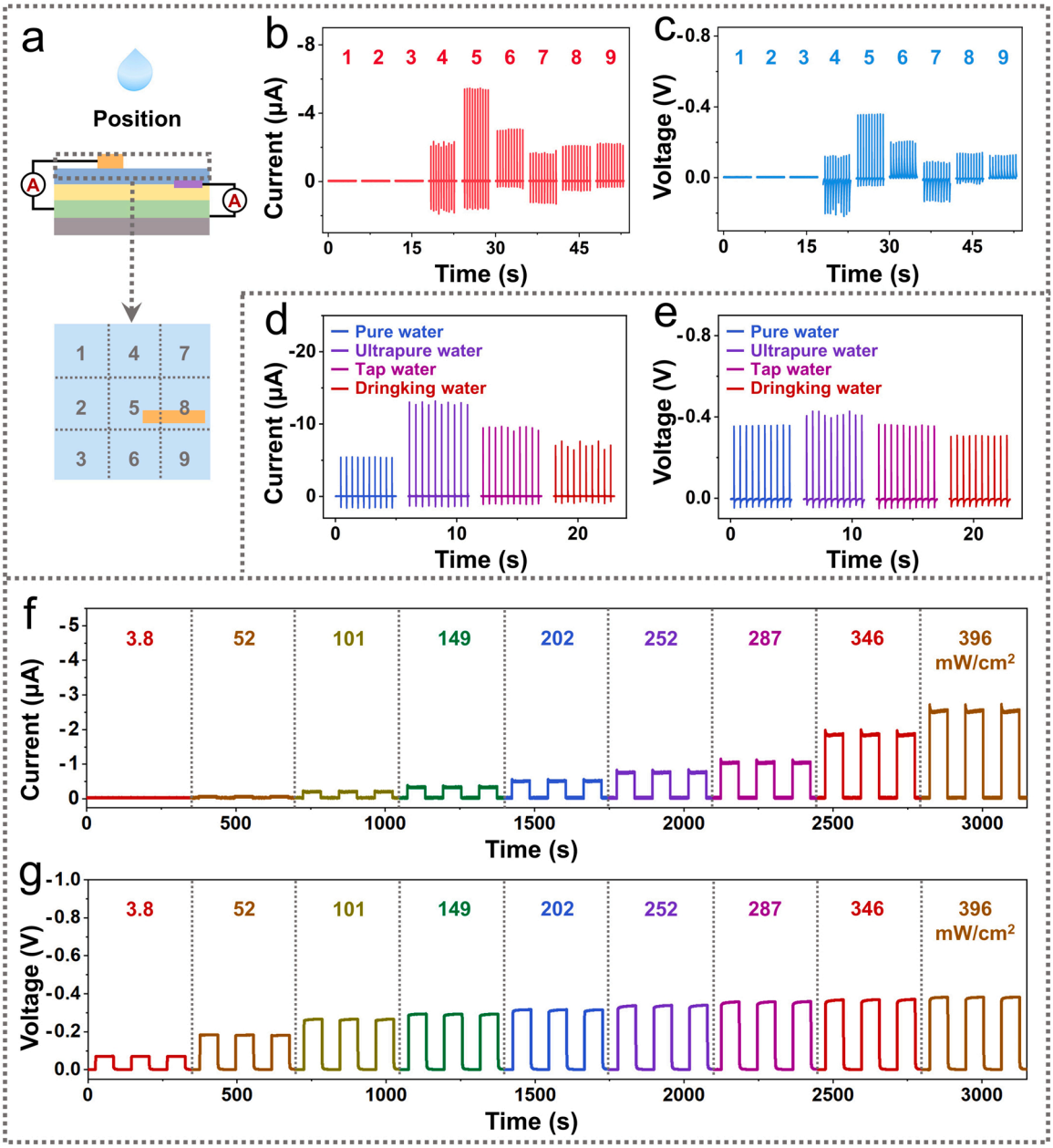

Fig. 5. Output performances of the device under different parameters. (a) The schematic diagram of the droplet dripping position. (Length of the Al electrode was 12 mm). (b) The output current and (c) voltage of the TENG under different dripping positions (height = 15 cm, size = 60 μL, frequency = 2 Hz, angle = 45°). (d) The output current and (e) voltage of the TENG with different water sources (height = 15 cm, size = 60 μL, frequency = 2 Hz, angle = 45°). (f) Light-induced current and (g) voltage of the PVC under 365 nm light illumination.

Fig. S7b,c, the best output occurs at compartment 5 either the Al electrode was 12 mm (Fig. 5a) or 30 mm (Fig. S7a). In addition, we found that different water sources made the test results difference, during the experiment. As shown in Fig. 5d,e, the output follows the order of pure water > tap water > salt solution > Ultra pure water. Fig. S6c-f show the output signals of the TENG under certain width and length of the Al electrode. Suggesting that the performance of the TENG is affected by neither width nor length of the Al electrode.

Considering that the light intensity and wavelength are main influencing factors of the PVC performance, the output signals under different light intensity and wavelength were measured. Fig. 5f,g show that the output current and voltage are positively correlated with light intensity. For the wavelength, the best output occur at 365 nm shown in Fig. S8a,b.

4. Conclusion

In summary, we developed a hybridized nanogenerator consisting of a PVC and a TENG, that can harvest both liquid-droplet energy and light energy. In particular, the BTO film was introduced to a liquid-droplet energy harvesting TENG, and was added between the bottom electrode and the friction layer to retain the surface charges, so that the output of the TENG could be improved. Moreover, the PVC could share the bottom electrode with the TENG, which could simplify the fabrication of the device. The device exhibited good hybridized effect, generating peak current of 16.96 μA and peak voltage of 0.83 V, during the sliding of a 100 μL pure water droplet from 50 cm height, on a 45° tilted device at a frequency of 4 Hz, with a 365 nm LED whose power density was 396 mW/cm^2 illuminating on the device. While the maximum peak power density could reach 3.71 mW/m^2 and the maximum output

energy density reached 15.36 mJ/m^2. The maximum hybridized peak power was determined by the maximum peak power of the TENG, while the maximum hybridized output energy was much more affected by the maximum output energy of the PVC, because the water droplet dropped down at a certain frequency made the TENG presents a pulselike output, while the output signals of the PVC was continuous. This work enables the simultaneously scavenging light and liquid-droplet energies through individual device, which will open up unexplored avenues for simultaneously scavenging liquid-droplet energy and other type of energies. Without being limited to a BTO film, one could speculate that many other materials might be used to scavenge other type of energies while work as an intermediate layer to improve the TENG performance also. In response to this idea, further research is needed, such as preparation of new materials, matching electric signals of two units of the device, clarification of the mechanism of the interaction of each unit.

CRediT authorship contribution statement

C.L., Z.L.W. and Y.Y. supervised the research and conceived the idea. C.B., H.D. and M.Z. carried out the device fabrication and the performance measurement. C.B., C.L., Z.L.W. and Y.Y. analyzed the data and co-wrote the manuscript. All authors read and revised the manuscript.

Declaration of Competing Interest

The authors declare that they have no known competing financial interests or personal relationships that could have appeared to influence the work reported in this paper.

Data Availability

Data will be made available on request.

Acknowledgments

This work was supported by the National Key R & D Project from Minister of Science and Technology in China (No. 2021YFA1201604), the National Natural Science Foundation of China (No. 52072041, 61974170), and the University of Chinese Academy of Sciences (Grant No. Y8540XX2D2).

Appendix A. Supporting information

Supplementary data associated with this article can be found in the online version at doi:10.1016/j.nanoen.2022.108063.

References

[1] F.R. Fan, Z.Q. Tian, Z.L. Wang, Flexible triboelectric generator, Nano Energy 1 (2012) 328–334.
[2] S.H. Wang, X. Wang, Z.L. Wang, Y. Yang, Efficient scavenging of solar and wind energies in a smart city, ACS Nano 10 (2016) 5696–5700.
[3] K. Liu, Z.L. Zhao, Y. Wang, Unity convoluted design of solid Li-ion battery and triboelectric nanogenerator for self-powered wearable electronics, Adv. Energy Mater. 7 (2017) 1701629.
[4] C.S. Wu, Aurelia C. Wang, W.B. Ding, H.Y. Guo, Z.L. Wang, Triboelectric nanogenerator: a foundation of the energy for the new era, Adv. Energy Mater. 9 (2019) 1802906.
[5] S. Lee, S.H. Bae, L. Lin, Flexible hybrid cell for simultaneously harvesting thermal and mechanical energies, Nano Energy 2 (2013) 817–825.
[6] Y. Yang. Hybridized and Coupled Nanogenerators. Design, Performance and Applications, Wiley-VCH GmbH, Weinheim, 2020.
[7] T. Quan, Y.C. Wu, Y. Yang, Hybrid electromagnetic-triboelectric nanogenerator for harvesting vibration energy, Nano Res. 8 (2015) 3272–3280.
[8] T. Quan, Y. Yang, Fully enclosed hybrid electromagnetic-triboelectric nanogenerator to scavenge vibrational energy, Nano Res. 9 (2016) 2226–2233.
[9] X. Chen, L.X. Gao, J.F. Chen, S. Lu, H. Zhou, T.T. Wang, A.B. Wang, Z.F. Zhang, S. F. Guo, X.J. Mu, Z.L. Wang, Y. Yang, A chaotic pendulum triboelectric-electromagnetic hybridized nanogenerator for wave energy scavenging and self-powered wireless sensing system, Nano Energy 69 (2020), 104440.
[10] T. Quan, Z.L. Wang, Y. Yang, A shared-electrode-based hybridized electromagnetic-triboelectric nanogenerator, ACS Appl. Mater. Interfaces 8 (2016) 19573–19578.
[11] B.J. Shi, Q. Zheng, W. Jiang, L. Yan, X.X. Wang, H. Liu, Y. Yao, Z. Li, Z.L. Wang, A packaged self-powered system with universal connectors based on hybridized nanogenerators, Adv. Mater. 28 (2016) 846–852.
[12] X. Wang, Z.L. Wang, Y. Yang, Hybridized nanogenerator for simultaneously scavenging mechanical and thermal energies by electromagnetic-triboelectric-thermoelectric effects, Nano Energy 26 (2016) 164.
[13] M. Salauddin, R.M. Toyabur, P. Maharjan, Design and experimental analysis of a low-frequency resonant hybridized nanogenerator with a wide bandwidth and high output power density, Nano Energy 66 (2019), 104122.
[14] M.T. Rahman, M. Salauddin, P. Maharjan, Natural wind-driven ultra-compact and highly efficient hybridized nanogenerator for self-sustained wireless environmental monitoring system, Nano Energy 57 (2019) 256.
[15] C. Hou, T. Chen, Y. Li, A rotational pendulum based electromagnetic-triboelectric hybrid-generator for ultra-low-frequency vibrations aiming at human motion and blue energy applications, Nano Energy 63 (2019), 103871.
[16] J.H. Nie, Z.M. Wang, Z.W. Ren, S.Y. Li, X.Y. Chen, Z.L. Wang, Power generation from the interaction of a liquid droplet and a liquid membrane, Nat. Commun. 10 (2019) 2264.
[17] J.Q. Xiong, G. Thangavel, J.X. Wang, X.R. Zhou, P.S. Lee, Self-healable sticky porous elastomer for gas-solid interacted power generation, Sci. Adv. 6 (2020) eabb4246.
[18] H.F. Qin, L. Xu, S.Q. Lin, F. Zhan, K. Dong, K. Han, H.M. Wang, Yw Feng, Z. L. Wang, Underwater energy harvesting and sensing by sweeping out the charges in an electric double layer using an oil droplet, Adv. Funct. Mater. 32 (2022) 2111662.
[19] Z.H. Lin, G. Cheng, S. Lee, K.C. Pradel, Z.L. Wang, Harvesting water drop energy by a sequential contact-electrification and electrostatic-induction process, Adv. Mater. 26 (2014) 4690–4696.
[20] W.H. Xu, H.X. Zheng, Y. Liu, X.F. Zhou, C. Zhang, Y.X. Song, X. Deng, M. Leung, Z. B. Yang, R.X. Xu, Z.L. Wang, X.C. Zeng, Z.K. Wang, A droplet-based electricity generator with high instantaneous power density, Nature 578 (2020) 392–396.
[21] Y. Chen, B. Xie, J.Y. Long, Y.C. Kuang, X. Chen, M.X. Hou, J. Gao, S. Zhou, B. Fan, Y.B. He, Y.T. Zhang, C.P. Wong, Zk Wang, N. Zhao, Interfacial laser-induced graphene enabling highperformance liquid−solid triboelectric nanogenerator, Adv. Mater. (2021) 2104290.
[22] Q. Zhang, C.M. Jiang, X.J. Li, S.F. Dai, Y.B. Ying, J.F. Ping, Highly efficient raindrop energy-based triboelectric nanogenerator for self-powered intelligent greenhouse, ACS Nano 15 (2021) 12314–12323.
[23] N. Tang, Y.B. Zheng, M.M. Yuan, K. Jin, H. Haick, High-performance polyimide-based water-solid triboelectric nanogenerator for hydropower harvesting, ACS Appl. Mater. Interfaces 13 (2021) 32106–32114.
[24] N. Zhang, H.J. Gu, K.Y. Lu, S.M. Ye, W.H. Xu, H.X. Zheng, Y.X. Song, C.R. Liu, J. W. Jiao, Z.K. Wang, X.F. Zhou, A universal single electrode droplet-based electricity generator (SE-DEG) for water kinetic energy harvesting, Nano Energy 82 (2021), 105735.
[25] J. Dong, C.Y. Xu, L.L. Zhu, X.S. Zhao, H.Y. Zhou, H.W. Liu, G.B. Xu, G. Wang, G. D. Zhou, Q.F. Zeng, Q.L. Song, A high voltage direct current droplet-based electricity generator inspired by thunderbolts, Nano Energy 90 (2021), 106567.
[26] X.T. Xu, Y.L. Wang, P.Y. Li, W.H. Xu, L. Wei, Z.K. Wang, Z.B. Yang, A leaf-mimic rain energy harvester by liquid-solid contact electrification and piezoelectricity, Nano Energy 90 (2021), 106573.
[27] L.J. Xie, L. Yin, Y.N. Liu, H.L. Liu, B.H. Lu, C. Zhao, T.A. Khattab, Z. Wen, X.H. Sun, Interface engineering for efficient raindrop solar cell, ACS Nano 16 (2022) 5292–5302.
[28] Li Zheng, Gang Cheng, Jun Chen, Long Lin, Jie Wang, Yongsheng Liu, Zhong Lin Wang, A hybridized power panel to simultaneously generate electricity from sunlight, rain drops and wind around the clock, Adv. Energy Mater. 5 (2015) 1501152.
[29] Li Zheng, Zong-Hong Lin, Gang Cheng, Wenzhuo Wu, Xiaonan Wen, Sangmin Lee, Zhong Lin Wang, Silicon-based hybrid cell for harvesting both solar energy and raindrop electrostatic energy, Nano Energy 9 (2014) 291–300.
[30] S.B. Jeon, D.W. Kim, G.W. Yoon, J.B. Yoon, Y.K. Choi, Self-cleaning hybrid energy harvester to generate power from raindrop and sunlight, Nano Energy 12 (2015) 636–645.
[31] Y.Q. Liu, N. Sun, J.W. Liu, Z. Wen, X.H. Sun, S.T. Lee, B.Q. Sun, Integrating silicon solar cell with triboelectric nanogenerator via a mutual electrode for harvesting energy from sunlight and raindrop, ACS Nano 12 (2018) 2893–2899.
[32] D.H. Yoo, S.C. Park, S.M. Lee, J.Y. Sim, I.S. Song, D.W. Choi, H.E. Lim, D.S. Kim, Biomimetic anti-reflective triboelectric nanogenerator for concurrent harvesting of solar and raindrop energies, Nano Energy 57 (2019) 424–431.
[33] X.L. Liu, K. Cheng, P. Cui, H. Qi, H.F. Qin, G.Q. Gu, W.Y. Shang, S.J. Wang, G. Cheng, Z.L. Du, Hybrid energy harvester with bi-functional nano-wrinkled anti-reflective PDMS film for enhancing energies conversion from sunlight and raindrops, Nano Energy 66 (2019), 104188.
[34] T.D. Lee, A.U. Ebong, A review of thin film solar cell technologies and challenges, Renew. Sustain. Energy Rev. 70 (2017) 1286–1297.
[35] Y. Ji, K.W. Zhang, Z.L. Wang, Y. Yang, Piezo-pyro-photoelectric effects induced coupling enhancement of charge quantity in $BaTiO_3$ materials for simultaneously scavenging light and vibration energies, Energy Environ. Sci. 12 (2019) 1231–1240.

[36] J.Z. Minhas, M.M. Hasan, Y. Yang, Ferroelectric materials based coupled nanogenerators, Nanoenergy Adv. 1 (2021) 131–180.
[37] K. Zhao, B.S. Ouyang, Y. Yang, Enhancing photocurrent of radially polarized ferroelectric $BaTiO_3$ materials by ferro-pyro-phototronic effect, iScience 3 (2018) 208–216.
[38] J. Wang, C.S. Wu, Y.J. Dai, Z.H. Zhao, A. Wang, T.J. Zhang, Z.L. Wang, Achieving ultrahigh triboelectric charge density for efficient energy harvesting, Nat. Commun. 8 (2017) 88.

Chengmin Bao is now studying for a doctor's degree. She is currently a visiting student in the research group of Professor Ya Yang at Beijing Institute of Nanoenergy and Nanosystems, Chinese Academy of Sciences. She obtained her bachelor's and master's degree in environmental science from Tianjin University in 2009 and 2012 respectively. Her current research interest is triboelectric nanogenerator and its application.

Huiyu Dan is pursuing his Ph.D. degree in Beijing Institute of Nanoenergy and Nanosystems, Chinese Academy of Sciences, China. He received his master's degree in School of Physical Science and Technology, Guangxi University in 2022. His current research interests include ferroelectric thin film materials and its applications.

Maoyi Zhang is pursuing his Ph.D. degree in Institute of Mechanics, Chinese Academy of Sciences, China. He received his bachelor's degree in Engineering Mechanics from Dalian University of Technology in 2017. His current research interests include flexible sensors and energy harvesters.

Prof. Chuanbo Li received his Ph.D. degree in Microelectronics & Solid State Electronics from Institute of Semiconductor, Chinese Academy of Science. He is currently a professor at Minzu University of China. He is mainly focusing on Si-based nanomaterial and nanodevices for nanoelectronics and clean energy application. He has published over 80 peer reviewed journal papers. He is the committees of IEEE GFP (2016), IEEE GFP2017, ECS AiMES 2018 (G03), ECS PRiME 2020 (G03). He is the associate Editor of Journal of Semiconductors. Details can be found at: http://www.researcherid.com/rid/A-1296–2009.

Prof. Zhong Lin (ZL) Wang received his Ph.D. from Arizona State University in physics. He now is the Hightower Chair in Materials Science and Engineering, Regents' Professor, Engineering Distinguished Professor and Director, Center for Nanostructure Characterization, at Georgia Tech. Dr. Wang has made original and innovative contributions to the synthesis, discovery, characterization and understanding of fundamental physical properties of oxide nanobelts and nanowires, as well as applications of nanowires in energy sciences, electronics, optoelectronics and biological science. His discovery and breakthroughs in developing nanogenerators established the principle and technological road map for harvesting mechanical energy from environment and biological systems for powering personal electronics. His research on self-powered nanosystems has inspired the worldwide effort in academia and industry for studying energy for micro-nano-systems, which is now a distinct disciplinary in energy research and future sensor networks. He coined and pioneered the field of piezotronics and piezophototronics by introducing piezoelectric potential gated charge transport process in fabricating new electronic and optoelectronic devices. Details can be found at: http:// www.nanoscience.gatech.edu.

Prof. Ya Yang received his Ph.D. in Materials Science and Engineering from University of Science and Technology Beijing, China. He is currently a professor at Beijing Institute of Nanoenergy and Nanosystems, Chinese Academy of Sciences, China. His main research interests focus on ferroelectric materials and devices for energy conversion, self-powered sensing, and some new physical effects. He has published one book and more than 220 SCI academic papers in Science Advances and other journals. These papers have been cited by more than 17000 times, and the corresponding H-index is 79. He is the Editor-in-Chief of Nanoenergy Advances and is the editorial committee member of InfoMat, Nano-Micro Letters, Nanoscale, iScience, Nanoscale Advances, and some other journals. He is the Guest Editor of Research, iScience, Nanomaterials, and Energies. Details can be found at: http://www.researcherid.com/rid/A-7219-2016.